

portant point for our work is that $\text{Cu}(\text{N}_3)_2$ is in no way a counterexample of the ability of the end-on azido bridges to favor a ground triplet state in copper(II) dinuclear complexes.

Registry No. $[\text{Cu}_2(t\text{-Bupy})_4(\text{N}_3)_2](\text{ClO}_4)_2$, 88200-68-4; $\text{Cu}(\text{N}_3)_2$,

14215-30-6.

Supplementary Material Available: Listings of structure factor amplitudes and magnetic data (17 pages). Ordering information is given on any current masthead page.

Contribution from the Chemistry Department, Manchester University, Manchester M13 9PL, England, and Department of Chemistry, The University of Arizona, Tucson, Arizona 85721

Crystal Structure and Spectroscopic Studies of $[\text{MoO}_2(\text{L-cysOMe})_2]$

IAIN BUCHANAN,^{1a} MARTIN MINELLI,^{1b} MICHAEL T. ASHBY,^{1b} TREVOR J. KING,^{1c} JOHN H. ENEMARK,^{*1b} and C. DAVID GARNER^{*1a}

Received April 22, 1983

$[\text{MoO}_2(\text{L-cysOMe})_2]$ crystallizes in the orthorhombic space group $P2_12_12$ with $a = 7.830$ (5), $b = 16.202$ (8), and $c = 5.861$ (3) Å, $V = 743.5$ Å³, $Z = 2$. The structure was solved by direct methods followed by least-squares refinement using 1065 independent reflections to a final R value of 0.038 ($R_w = 0.054$). The molecules have crystallographic C_2 symmetry and possess the expected *cis*-dioxo ($\text{Mo}-\text{O} = 1.714$ (4) Å), *trans*-dithiolate ($\text{Mo}-\text{S} = 2.414$ (2) Å), and *cis*-diamino ($\text{Mo}-\text{N} = 2.375$ (5) Å) distorted octahedral configurations. The molecules crystallize with the Λ configuration at the metal, and the L-cysteine chelate rings have the λ conformation. $[\text{MoO}_2(\text{L-cysOMe})_2]$ exists as two isomers in solution, as observed by ¹H, ¹³C, and ⁹⁵Mo NMR spectroscopy; these are assigned as the Λ and Δ diastereomers of the $\text{MoO}_2(\text{S},\text{N})_2$ complex and appear in relative amounts of ca. 5:1. Interconversion between these diastereomers has been observed by ⁹⁵Mo NMR spectroscopy. Coalescence of the two signals occurs at ca. 333 K and thus ΔG^\ddagger for the isomerization process is ca. 64 kJ mol⁻¹. The circular dichroism spectrum of $[\text{MoO}_2(\text{L-cysOMe})_2]$ resolves each of the two bands of the UV-visible spectrum (at ca. 352 and 259 nm) into two components at 413/353 and 284/268 nm.

Introduction

The pursuit of chemical analogues of the molybdenum centers of the molybdoenzymes has led to significant developments in the synthesis and characterization of molybdenum complexes.² Measurement of the extended X-ray absorption fine structure (EXAFS) associated with the molybdenum K edge has provided direct evidence concerning the nature, number, and distance of the ligand donor atoms coordinated to molybdenum in several of these enzymes.³⁻⁶ In the oxidized form of the molybdoenzymes which catalyze net oxygen-atom transfer reactions, the (presumed) molybdenum(VI) center is bound to one or more oxo groups and several sulfur ligands. In the specific instance of chicken liver sulfite oxidase, molybdenum(VI) appears to be coordinated to two oxo groups ($\text{Mo}-\text{O} = \text{ca. } 1.68$ Å) and two or three sulfur atoms ($\text{Mo}-\text{S} = \text{ca. } 2.41$ Å). Chemical systems that possess oxo and sulfur coordination of molybdenum(VI) include the cysteine ester complexes, $[\text{MoO}_2(\text{cysOR})_2]$, which have been known for some time, particularly for $\text{R} = \text{Me}$ or Et .^{7,8} However, a com-

prehensive characterization of these complexes has not been reported. Therefore, we have investigated the structure and spectroscopic properties of these systems. Herein we report the crystal structure of $[\text{MoO}_2(\text{L-cysOMe})_2]$ and some spectroscopic properties of this and the corresponding ethyl ester derivative. These studies were also stimulated by the chiral nature of the molybdenum center in complexes of this type, with reference to the circular dichroism (CD) properties of the molybdenum domain of sulfite oxidase,⁹ and the desire to further demonstrate the sensitivity of ⁹⁵Mo NMR spectroscopy, for example, to distinguish between diastereomeric complexes.¹⁰

Experimental Section

Preparation of the Compounds. The ligands methyl and ethyl L-cysteinate were obtained as their hydrochlorides from Sigma. $[\text{MoO}_2(\text{L-cysOR})_2]$ ($\text{R} = \text{Me}$ or Et) was prepared according to previously published procedures.^{7,8} Anal. Calcd for $\text{C}_8\text{H}_{16}\text{N}_2\text{MoO}_6\text{S}_2$ ($\text{R} = \text{Me}$): C, 24.2; H, 4.1; N, 7.1; Mo, 24.2. Found: C, 24.1; H, 4.0; N, 7.0; Mo, 23.1. Calcd for $\text{C}_{10}\text{H}_{20}\text{N}_2\text{MoO}_6\text{S}_2$ ($\text{R} = \text{Et}$): C, 28.3; H, 4.8; N, 6.6; Mo, 22.6. Found: C, 28.7; H, 5.0; N, 6.3; Mo, 22.4. Crystals of $[\text{MoO}_2(\text{L-cysOMe})_2]$ suitable for structure determination by X-ray crystallography were obtained by slow evaporation in air of a solution containing the compound dissolved in ethyl acetate. The crystals were obtained as yellow needles, which showed well-defined optical anisotropy to transmitted light when viewed through a polarizing microscope, being yellow when viewed in one orientation and green when viewed perpendicular to this.

X-ray Structure Determination. A well-formed crystal was mounted on a Syntex P2₁ autodiffractometer equipped with a scintillation counter and a graphite monochromator. The longest dimension of the crystal was approximately parallel to the ϕ axis. The results from the automatic centering, indexing, and least-squares routines and the axial photographs were consistent with a primitive orthorhombic lattice. Data were collected for the hkl octant and reduced to F_o^2 and $\sigma(F_o^2)$

(1) (a) Manchester University; (b) The University of Arizona; (c) The Chemistry Department, Nottingham University, Nottingham NG7 2RD, England.

(2) Reviews: Stiefel, E. I. *Prog. Inorg. Chem.* 1977, 22, 1. "Molybdenum Chemistry of Biological Significance"; Newton, W. E., Otsuka, S., Eds.; Plenum Press: New York, 1980. "Molybdenum and Molybdenum-Containing Enzymes"; Coughlan, M. P., Ed.; Pergamon Press: New York, 1980. Garner, C. D. *Coord. Chem. Rev.* 1981, 37, 117; 1982, 45, 153. Müller, A.; Jaegermann, W.; Enemark, J. H. *Ibid.* 1982, 46, 245.

(3) Cramer, S. P.; Gray, H. B.; Rajagopalan, K. V. *J. Am. Chem. Soc.* 1979, 101, 2772. Cramer, S. P.; Wahl, R.; Rajagopalan, K. V. *Ibid.* 1981, 103, 7721.

(4) Bordas, J.; Bray, R. C.; Garner, C. D.; Gutteridge, S.; Hasnain, S. S. *J. Inorg. Biochem.* 1979, 11, 181. Bordas, J.; Bray, R. C.; Garner, C. D.; Gutteridge, S.; Hasnain, S. S. *Biochem. J.* 1980, 191, 499.

(5) Tullius, T. D.; Kurtz, D. M., Jr.; Conradson, S. D.; Hodgson, K. O. *J. Am. Chem. Soc.* 1979, 101, 2776.

(6) Cramer, S. P.; Hodgson, K. O.; Gillum, W. O.; Mortenson, L. E. *J. Am. Chem. Soc.* 1978, 100, 3398. Cramer, S. P.; Gillum, W. O.; Hodgson, K. O.; Mortenson, L. E.; Stiefel, E. I.; Chisnell, J. R.; Brill, W. J.; Shah, V. K. *Ibid.* 1978, 100, 3814.

(7) Melby, L. R. *Inorg. Chem.* 1969, 8, 349.

(8) Kay, A.; Mitchell, P. C. H. *J. Chem. Soc. A* 1970, 2421.

(9) Garner, C. D.; Buchanan, I.; Collison, D.; Mabbs, F. E.; Porter, T. G.; Wynn, C. H. "Proceedings of the Fourth International Conference on the Chemistry and Uses of Molybdenum"; Mitchell, P. C. H., Barry, H., Eds.; Climax Molybdenum Co.: Golden, CO, 1982.

(10) Minelli, M.; Rockway, T. W.; Enemark, J. H.; Brunner, H.; Muschiol, M. *J. Organomet. Chem.* 1981, 217, C34.

Table I. Crystallographic Data for Λ -[MoO₂(L-cysOMe)₂] at 25 °C^a

formula	C ₈ H ₁₆ O ₆ N ₂ S ₂ Mo
<i>M_r</i>	396.30
space group	<i>P</i> 2 ₁ 2 ₁ 2 (No. 18)
cell dimens	
<i>a</i> , Å	7.830 (5)
<i>b</i> , Å	16.202 (8)
<i>c</i> , Å	5.861 (3)
<i>V</i> , Å ³	743.5
<i>Z</i>	2
<i>d</i> _{calcd.} , g cm ⁻³	1.770
cryst shape	hexagonal needle
cryst dimens, mm	0.10 × 0.10 × 0.41
abs coeff, cm ⁻¹	12.7
radiation, Å	λ(Mo Kα) 0.71073
monochromator	graphite crystal
supplied power	50 kV, 25 mA
data collection method	θ-2θ scan
scan speed, deg min ⁻¹	variable (2.0–29.3 in the range 2° < 2θ < 50°), determined as a function of peak intensity
scan range (2θ), deg	Mo Kα ₁ -0.8 to Mo Kα ₂ +0.8
ratio of total bkgd time to peak scan time	0.5
std reflns	(003), (400), (060), after every 97 readings
std dev of stds	<2%
2θ limit, deg	2–50
no. of unique data	1467
no. of data used in the calcs	1065, <i>I</i> > 3σ(<i>I</i>)

^a The standard deviation of the least significant figure is given in the parentheses in this and subsequent tables.

by procedures previously described.¹¹ Lorentz-polarization factors were calculated on the assumption of 50% mosaicity and 50% perfection of the monochromator crystal. The systematic absences *0k0* for *k* = 2*n* + 1 and *00l* for *l* = 2*n* + 1 were consistent with the nonstandard space group *P*2₁2₁. Applying the matrix

$$\begin{bmatrix} h' \\ k' \\ l' \end{bmatrix} = \begin{bmatrix} 0 & 1 & 0 \\ 0 & 0 & 1 \\ 1 & 0 & 0 \end{bmatrix} \begin{bmatrix} h \\ k \\ l \end{bmatrix}$$

transformed the data and cell constants into *P*2₁2₁2 (No. 18), the standard setting. Table I lists crystallographic details. No absorption correction was applied.

The structure was solved by direct methods¹² using the 220 reflections with the largest values of *|E|*. The initial *E*-map revealed positions of six of the nine non-hydrogen atoms. The three remaining carbon and oxygen atoms were located in the first difference electron density map.

Least-squares refinement was based upon the 1065 reflections having *F*_o² ≥ 3σ(*F*_o²). The quantity minimized was Σ*w*(*|F*_o - *|F*_c)², where *w* = 4*F*_o²/σ(*F*_o²). Neutral atomic scattering factors were used for all non-hydrogen atoms;¹³ the values of Stuart, Davidson, and Simpson¹⁴ were used for hydrogen atoms. The effects of the real and imaginary components of anomalous dispersion for the molybdenum and sulfur atoms were included in the structure factor calculations by using the tabulated values of Cromer.¹⁵ Anisotropic refinement of all non-hydrogen atoms gave *R* = Σ||*F*_o - *|F*_c||/Σ|*F*_o| = 0.056 and *R*_w = [Σ*w*(*|F*_o - *|F*_c)²/Σ*wF*_o²]^{1/2} = 0.080. A difference electron density map revealed the hydrogen atoms bound to the nitrogen atom but did not show positions for hydrogen atoms bound to carbon atoms. The hydrogen atoms attached to C1 and C2 were included as fixed contributions assuming idealized tetrahedral geometry at these carbon atoms and C-H = 0.95 Å.¹⁶ Each hydrogen atom was assigned an

Table II. Atomic Coordinates for Λ -[MoO₂(L-cysOMe)₂]

atom	<i>x</i>	<i>y</i>	<i>z</i>
Mo	0.500000 (0)	0.500000 (0)	0.76913 (9)
S	0.53848 (20)	0.64445 (9)	0.85598 (29)
O	0.3229 (6)	0.5022 (4)	0.5974 (6)
O1	-0.0177 (8)	0.6003 (4)	1.1331 (11)
O2	0.0988 (6)	0.66144 (29)	1.4380 (8)
N	0.3086 (6)	0.52223 (29)	1.0775 (8)
C1	0.3277 (8)	0.6661 (4)	0.9671 (11)
C2	0.2872 (8)	0.6070 (4)	1.1614 (10)
C3	0.1044 (8)	0.6197 (4)	1.2415 (13)
C4	-0.0752 (10)	0.6781 (5)	1.5266 (16)

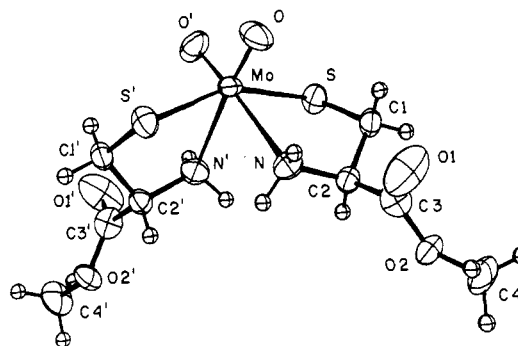


Figure 1. Structure of Λ -[MoO₂(cysOMe)₂] viewed down a pseudo-3-fold axis of the distorted octahedron illustrating the Λ configuration about the molybdenum atom and the λ conformations of the chelate rings.

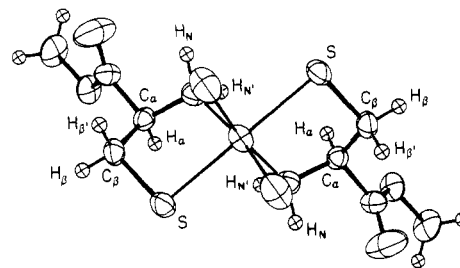


Figure 2. Projection down the *C*₂ axis of Λ -[MoO₂(L-cysOMe)₂] showing the angular distortion from octahedral geometry, i.e., the nonclipped positions of the O and N atoms, and the spectroscopically distinct C and H atoms.

isotropic temperature factor 1 Å² greater than the atom to which it was bonded. Refinement converged with *R*₁ = 0.038, *R*₂ = 0.054, and GOF = [Σ*w*(*|F*_o - *|F*_c)²/(*n* - *m*)]^{1/2} = 2.887. The largest residual in the final difference electron density map (1.31 e Å⁻³) was located between the molybdenum atom and the terminal oxygen atom.

The absolute configuration of the complex was assumed to be that which maintained the L-configuration of the ligand. As an independent check of the stereochemistry, the coordinates of the atoms were inverted and the alternative isomer refined to give *R*₁ = 0.039 and *R*₂ = 0.055. An *R*-factor ratio test¹⁷ indicated that the alternative stereochemistry could be rejected at the 95% confidence level.

Final positional parameters are given in Table II. Anisotropic thermal parameters, hydrogen atom positions, and a list of *|F*_o and *|F*_c are available as supplementary material.

Spectroscopic Measurements. UV-visible spectra were recorded on a Perkin-Elmer 402 spectrometer and CD spectra were obtained by using a Cary 61 Circular Dichrograph spectrometer calibrated with *d*-camphor-10-sulfuric acid. ⁹⁵Mo NMR spectra were recorded at 16.3 MHz for solutions dissolved in DMF at temperatures between 293 and 333 K on a Bruker WM 250 NMR spectrometer equipped with a 15-mm broad-band probe capable of operating from 10 to 35 MHz. The 90° pulse for ⁹⁵Mo was found to be 125 μs. For these studies pulse widths of 20–30 μs were used to give adequate power distribution over the 50-kHz spectral width. A data table of 4K or

- (11) Yamanouchi, K.; Enemark, J. H. *Inorg. Chem.* **1978**, *17*, 1981.
- (12) Germain, G.; Main, P.; Woolfson, M. M. *Acta Crystallogr., Sect. B* **1971**, *27*, 368.
- (13) "International Tables for X-ray Crystallography"; Kynoch Press: Birmingham, England, 1974; Vol. IV.
- (14) Stuart, R. F.; Davidson, E. R.; Simpson, W. T. *J. Chem. Phys.* **1965**, *42*, 3175.
- (15) Cromer, D. T. *Acta Crystallogr.* **1965**, *18*, 17.
- (16) Churchill, M. R. *Inorg. Chem.* **1973**, *12*, 1213.

- (17) Hamilton, W. C. "Statistics in Physical Sciences"; Ronald Press: New York, 1964; pp 157–162.

Table III. Selected Interatomic Distances (Å) in Λ -[MoO₂(L-cysOMe)₂]

Mo-O	1.714 (4)	C1-C2	1.521 (9)
Mo-N	2.375 (5)	C2-C3	1.521 (8)
Mo-S	2.414 (2)	C3-O1	1.190 (9)
S-Cl	1.808 (6)	C3-O2	1.336 (9)
N-C2	1.469 (8)	O2-C4	1.483 (7)

Table IV. Selected Interatomic Angles (deg) in Λ -[MoO₂(L-cysOMe)₂]^a

O-Mo-O'	108.1 (3)	C1-S-Mo	98.6 (2)
O-Mo-N	86.2 (2)	C2-N-Mo	117.9 (4)
O-Mo-N'	163.8 (2)	S-Cl-C2	109.8 (4)
O-Mo-S	101.8 (2)	N-C2-C1	108.3 (5)
O-Mo-S'	92.5 (2)	N-C2-C3	109.7 (5)
N-Mo-N'	80.9 (3)	C1-C2-C3	110.0 (5)
N-Mo-S	76.8 (1)	O1-C3-O2	124.6 (6)
N-Mo-S'	84.7 (1)	O1-C3-C2	123.7 (6)
S-Mo-S'	155.65 (9)	O2-C3-C2	111.5 (5)
		C3-O2-C4	115.1 (5)

^a Primed atoms are related to unprimed atoms by the 2-fold axis through the Mo atom.

8K points was used in collection. The digital resolution was 1.5 ppm for 4K spectra. An acquisition delay of 200 μ s was used to reduce the effects of probe ringing. Additional data points were shifted from the free induction decay (FID) as necessary to obtain a maximum total of 400 μ s. All spectra were recorded without field-frequency lock. The position of the external standard (2 M Na₂MoO₄ in H₂O at pH 11) was checked before and after each spectrum. No appreciable drift of the field was observed. Solution concentrations were usually 0.1 M.

Fourier transform ¹H and ¹³C NMR spectra were recorded at 400 and 100 MHz, respectively, using the S.E.R.C. facility at Sheffield University, or at 300 (Varian SC300 instrument) and 20 MHz (Bruker WP80 instrument), respectively, at Manchester University. Chemical shifts are reported in ppm downfield of Me₄Si.

Results and Discussion

Description of Structure. Perspective views of the structure of Λ -[MoO₂(L-cysOMe)₂]¹⁸ are shown in Figures 1 and 2, and pertinent interatomic dimensions are summarized in Table III and IV. The molecule has crystallographic C₂ symmetry.

Several six-coordinate dioxomolybdenum(VI) complexes in which the MoO₂²⁺ core is lighted by two thiolate groups and two amine nitrogen atoms of bidentate or tetradentate ligands have been structurally characterized in recent years.¹⁹⁻²³ These complexes exhibit two general types of distorted coordination geometries.²² The most common structural type involves a distorted octahedral geometry, with cis oxo groups, trans thiolate groups, and cis amine groups; thus, the amine nitrogen atoms are approximately trans to the oxo groups. Such an arrangement of ligands is found here for Λ -[MoO₂(L-cysOMe)₂], with the distances, Mo-O = 1.714 (4), Mo-N = 2.375 (5), and Mo-S = 2.414 (2) Å, being in the ranges tabulated previously²² for this group of complexes: Mo-O = 1.677-1.750, Mo-N = 2.357-2.486, and Mo-S = 2.408-2.429 Å.

The values obtained for the length of the Mo-O and Mo-N bonds of [MoO₂(L-cysOEt)₂] in an earlier EXAFS study⁴ (1.74 and 2.38 Å, respectively) are in good accord with the crystallographic values; however, the Mo-S bond length was estimated to be longer by ca. 0.07 Å in this EXAFS study.

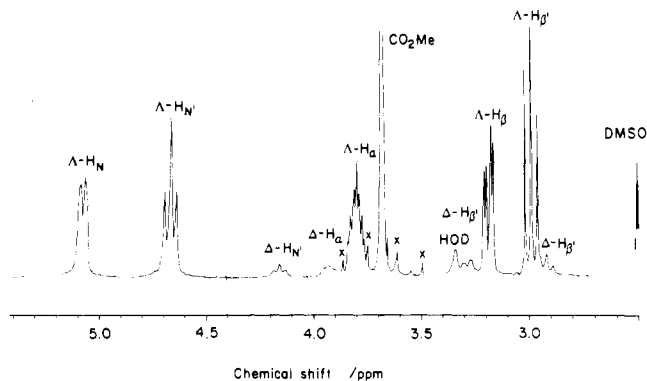


Figure 3. ¹H NMR spectrum of [MoO₂(L-cysOMe)₂] recorded at 400 MHz in Me₂SO-*d*₆ at 24 °C (X = spinning side bands; see text for description and discussion of assignments).

Also, we note that the Mo-O and Mo-S distances, of 1.68 and 2.41 Å, respectively, obtained from EXAFS data for sulfite oxidase³ are typical of *cis*-dioxomolybdenum(VI) complexes and, as such, have a reasonably good correspondence to the values obtained in this study.

The distorted octahedral arrangement of the ligand donor atoms about the molybdenum is also manifest in the bond angles; for example, O-Mo-S = 101.8 (2)°, O-Mo-S' = 92.5 (2)° (see Figure 2), and S-Mo-S' = 155.7 (1)°. Similar distortions occur for other MoO₂(S₂N₂) complexes²² and have been rationalized on the basis of nonbonded repulsions among the donor atoms.^{20,24}

The chelate rings adopt the λ conformation¹⁸ with the bulky -CO₂Me group in the sterically less crowded equatorial position. It is interesting to compare this overall stereochemistry ($\Delta\lambda\lambda$ -L-cysOMe) with that found in the solid state²³ for [MoO₂(D-penOMe)₂] (pen = penicillamine; the D-penOMe ligand has the opposite stereochemistry from L-cysOMe at C_α and contains two Me groups at C_β (Figure 2)). [MoO₂(D-penOMe)₂] crystallizes as a 1:1 mixture of Λ and Δ isomers. The overall stereochemistry of the Δ isomer is $\Delta\delta\delta$ -D-penOMe; *i.e.*, all elements of chirality are inverted with respect to those found here ($\Delta\lambda\lambda$ -L-cysOMe). The bulky -CO₂Me group occupies an equatorial position. For Λ -[MoO₂(D-penOMe)₂] the -CO₂Me group again occupies an equatorial position. This means that the chelate rings remain in the δ configuration and that the overall stereochemistry is ($\Delta\delta\delta$ -D-penOMe). From the structural results for [MoO₂(D-penOMe)₂] complexes,²³ it seems likely that the minor conformer observed in solution for [MoO₂(L-cysOMe)₂] (*vide infra*) has the overall stereochemistry ($\Delta\lambda\lambda$ -L-cysOMe) and differs from the major isomer only in the configuration at the molybdenum atom.

Each of the amino protons is involved in one intermolecular hydrogen bond in the crystal structure. The HN1 proton is weakly hydrogen bonded to a terminal oxo group (N...O = 3.07 Å, N-H...O = 131°), and the HN2 proton is hydrogen bonded to a carboxyl oxygen atom (N...O = 2.26 Å, N-H...O = 137°).

NMR Spectra: (i) ¹H Spectra. The 400-MHz ¹H NMR spectrum of Λ -[MoO₂(L-cysOMe)₂], dissolved in Me₂SO-*d*₆ at 24 °C, is reproduced in Figure 3 and the details, together with those of the corresponding ethyl ester complex, are summarized in Table V. Six major sets of peaks are observed in this spectrum, corresponding to the six proton environments on each methyl ester ligand in this complex (Figure 2). These are the ester -OMe group (3.68 ppm, singlet, with ca. three times the intensity of the other resonances), the α -proton (H_α: 3.80 ppm, multiplet), the β -CH₂ (H_β: 3.17 ppm, quartet, H_β': 2.98 ppm, triplet), and amine (H_N: 5.08 ppm, doublet; H_N':

(18) IUPAC Commission on the Nomenclature of Inorganic Chemistry. *Pure Appl. Chem.* **1971**, *28*, 1.

(19) Berg, J. M.; Hodgson, K. O.; Cramer, S. P.; Corbin, J. L.; Elsberry, A.; Pariyadath, N.; Stiefel, E. I. *J. Am. Chem. Soc.* **1979**, *101*, 2774.

(20) Yamanouchi, K.; Enemark, J. H. *Inorg. Chem.* **1979**, *18*, 1926.

(21) Stiefel, E. I.; Miller, K. F.; Bruce, A. E.; Corbin, J. L.; Berg, J. M.; Hodgson, K. O. *J. Am. Chem. Soc.* **1980**, *102*, 3624.

(22) Bruce, A.; Corbin, J. L.; Dahlstrom, P. L.; Hyde, J. R.; Minelli, M.; Stiefel, E. I.; Spence, J. T.; Zubietta, J. *Inorg. Chem.* **1982**, *21*, 917.

(23) Buchanan, I.; Clegg, W.; Garner, C. D., submitted for publication.

(24) Kepert, D. L. *Prog. Inorg. Chem.* **1977**, *23*, 1.

Table V. ^1H NMR Data^a for $[\text{MoO}_2(\text{L-cysOR})_2]$ (R = Me or Et) Complexes^b

	Λ - $[\text{MoO}_2(\text{L-cysOMe})_2]$ ^c	Δ - $[\text{MoO}_2(\text{L-cysOMe})_2]$ ^c	Λ - $[\text{MoO}_2(\text{L-cysOEt})_2]$ ^d
H_α	3.80 ^e	3.93 ^e	3.81 ^e
H_β	3.17 q	3.29 q	3.19 q
$\text{H}_{\beta'}$	2.98 t	2.92 t	3.01 t
H_N	5.08 d	ca. 4.6	5.10 d
$\text{H}_{\text{N}'}$	4.58 t	4.16 t	4.62 t
R	3.68 s	3.69 ^g	4.15 q, 1.21 t
$^2J_{\beta,\beta'}$	12.3	ca. 12	12.2
$^3J_{\alpha,\beta}$	4.4	ca. 4	4.4
$^3J_{\alpha,\beta'}$	11.2	ca. 12	10.4
$^2J_{\text{N},\text{N}'}$	9.0	ca. 10	8.5
$^3J_{\alpha,\text{N}}$	f	f	f
$^3J_{\alpha,\text{N}'}$	12.0	ca. 10	12.5
J_R			6.8

^a Recorded in $\text{Me}_2\text{SO}-d_6$ at 24 °C. Coupling constants in Hz. See Figure 2: H_α bonded to C2; H_β and $\text{H}_{\beta'}$ bonded to C1; H_N and $\text{H}_{\text{N}'}$ bonded to N, but note that the assignments of H_N vs. $\text{H}_{\text{N}'}$ and H_β vs. $\text{H}_{\beta'}$ on this figure are tentative. Chemical shift on δ scale referenced to Me_4Si . ^b Cf. 60-MHz data for $\text{cysOR}\cdot\text{HCl}$ in $\text{CF}_3\text{CO}_2\text{H}$ at 24 °C: R = Me, Et; H_α , 4.65 (t, $J = 5.3$), 4.68 (t, $J = 5.3$); H_β , 3.33 (m), 3.36 (m); H_N , 7.5 (s, broad), 7.5 (s, broad); $\text{H}_{\beta'}$, 1.77 (t, $J = 8.7$), 1.84 (t, $J = 9.3$); R, 4.02 (s), 4.47 and 1.40 (q and t, $J = 7.3$). ^c 400-MHz data. ^d 300-MHz data. ^e s = singlet, d = doublet, t = triplet, q = quartet, m = multiplet. ^f Not resolved. ^g Resonance assigned as the shoulder of the corresponding resonance of Λ -diastereomer.

4.58 ppm, triplet) protons. On decoupling of the α -proton resonance, the β -proton and amine proton regions simplify to AB quartets, with geminal coupling constants of $^2J_{\beta,\beta'}$ (between H_β and $\text{H}_{\beta'}$) of 12.3 Hz and $^2J_{\text{N},\text{N}'}$ (between H_N and $\text{H}_{\text{N}'}$) of 9.0 Hz. Assuming first-order splitting, the separation of the two outermost lines of any resonance equals the sum of the geminal and vicinal coupling constants. Thus, it is possible to measure the coupling constants involving H_α : $^3J_{\alpha,\beta} = 4.4$, $^3J_{\alpha,\beta'} = 11.2$, $^3J_{\alpha,\text{N}} = 12.0$ Hz. However, the coupling of H_α to H_N was not resolved, and the H_N resonance appears as a doublet. Since the two coupling constants involving $\text{H}_{\beta'}$ ($^2J_{\beta,\beta'} = 12.3$, $^3J_{\alpha,\beta'} = 11.2$ Hz) are very similar, the $\text{H}_{\beta'}$ resonance appears as a triplet, in contrast to the four-line pattern observed for H_β . Similarly, the $\text{H}_{\text{N}'}$ amine proton resonance is manifest as a triplet ($^2J_{\text{N},\text{N}'} = 9.0$, $^3J_{\alpha,\text{N}'} = 12.0$ Hz).

Close inspection of the ^1H NMR spectrum of $[\text{MoO}_2(\text{L-cysOMe})_2]$ (Figure 3) reveals further weak resonances in (i) the β -proton region (2.92 ppm, triplet; 3.29 ppm, quartet), (ii) the α -proton region (3.93 ppm, multiplet), and (iii) the amine proton region (4.16 ppm, triplet). These resonances appear to be quite reproducible and are considered to belong to a second cysteine methyl ester complex. The methyl ester $-\text{OMe}$ resonance is considered to appear as a shoulder to low field (3.69 ppm) of the analogous resonance of the major species. Integration of the spectrum suggests a relative ratio of ca. 5:1 for the major and minor species. Although only one extra amine proton resonance is observed, integration of the H_N and $\text{H}_{\text{N}'}$ peaks of the major species leads to the ratio 5:6, suggesting that the second amine resonance is obscured below the $\text{H}_{\text{N}'}$ resonance. Approximate coupling constants have been obtained for this minority species: $^2J_{\beta,\beta'} \sim ^3J_{\alpha,\beta'} \sim 12$, $^3J_{\alpha,\beta} \sim 4$, $^2J_{\alpha,\text{N}'} \sim 10$ Hz.

The addition of D_2O to a solution of $[\text{MoO}_2(\text{L-cysOMe})_2]$ in $\text{Me}_2\text{SO}-d_6$ causes the disappearance of all of the amine proton resonances. This is not unexpected, but it is of interest with respect to the proton which is exchangeable with water on the molybdenum(V) centers of the molybdoenzymes, detected by EPR spectroscopy.²⁵

The 300-MHz NMR spectrum of $[\text{MoO}_2(\text{L-cysOEt})_2]$ (Table V) is very similar to that of the methyl ester complex, except that the $-\text{OMe}$ resonance at 3.68 ppm is replaced by a quartet (4.15 ppm) and triplet (1.21 ppm) assigned to the methylene and methyl protons, respectively, of the $-\text{OEt}$ groups. The coupling between these resonances is 6.8 Hz. However, unlike $[\text{MoO}_2(\text{L-cysOMe})_2]$ for which a minority species was observed at 400 and 300 MHz, signals due to a second solution constituent were not definitely apparent.

The assignment of the major isomer of $[\text{MoO}_2(\text{L-cysOMe})_2]$ as Λ is based, primarily, upon the crystallographic results, which indicate that this is the only form present in the solid phase. This interpretation receives corroboration from data obtained²³ for $[\text{MoO}_2(\text{D-penOMe})_2]$. As indicated above, the solid exists as a 1:1 mixture of Λ and Δ isomers, and solutions exhibit ^1H and ^{13}C NMR spectra consistent with these isomers having comparable stabilities. The single isomer identified by ^1H NMR spectroscopy for $[\text{MoO}_2(\text{L-cysOEt})_2]$ is assigned as the Δ diastereomer in light of the data for the methyl ester. This assignment is consistent with the CD results (vide infra).

The ^1H NMR spectra of $[\text{MoO}_2(\text{L-cysOMe})_2]$ and $[\text{MoO}_2(\text{L-cysOEt})_2]$ are consistent with the previously reported spectra of cysteine and cysteine ester complexes.²⁶ Two major changes in the ^1H NMR spectra are observed to occur in going from $\text{L-cysOR}\cdot\text{HCl}$ (R = Me or Et) (in $\text{CF}_3\text{CO}_2\text{H}$ at 24 °C) to the corresponding $[\text{MoO}_2(\text{L-cysOR})_2]$ complex (in $\text{Me}_2\text{SO}-d_6$ at 24 °C): (i) the amine proton resonances become sharper, split into two regions, as expected from inspection of Figure 2, and are displaced 2.0–3.5 ppm upfield; (ii) the H_α multiplet is shifted ca. 0.9 ppm upfield. The upfield shift of the amine proton resonances is taken to indicate that, in these complexes, molybdenum is a weaker Lewis acid than the proton; i.e., the comparison is between $-\text{NH}_2\text{-Mo}$ and $-\text{NH}_3^+$. This effect appears to extend to the adjacent H_α atom, presumably by induction. The phenomenon is much less marked for the H_{β} -protons of the cysteine ester ligands, suggesting that the ability of molybdenum to act as a Lewis acid to sulfur is roughly comparable to that of the proton. This difference in the relative Lewis acidities of molybdenum(VI) and the proton for nitrogen and sulfur donor atoms may arise from the trans-weakening influence of the terminal oxo ligands; i.e., positions trans to terminal oxo-ligands, where the amino groups are bound, are rendered weaker electron acceptors than the positions cis to these oxo groups, which are occupied by the thiolates.

Since the positions of the hydrogen atoms, apart from those of the amine group, were not located in this study, no definite comments can be made concerning the magnitude of the vicinal coupling constants, 3J . By the use of relationship 1²⁷ the

$$^3J \sim 10 \cos^2 \theta \quad (1)$$

coupling constants $^3J_{\alpha,\text{N}}$ and $^3J_{\alpha,\text{N}'}$ are calculated from the NH_2 and C_αH positions as 6.8 and 7.5 Hz. The values of 12.0 and ca. 0 observed suggest that the chelate ring adopts a significantly different conformation in Me_2SO solution as compared to the crystal lattice, possibly due to changes in the hydrogen bonding interactions of the NH protons.

The large chemical shift difference between H_N and $\text{H}_{\text{N}'}$ (~ 0.5 ppm) is consistent with the very different chemical environments for these two protons (Figures 1 and 2). One of these protons, tentatively assigned as H_N , is adjacent to a

- (26) Martin, R. B.; Mathur, R. J. *J. Am. Chem. Soc.* **1965**, *87*, 1065. Matusch, D. F. S.; Porter, L. J. *J. Chem. Soc. A* **1971**, 2527. Kay, A.; Mitchell, P. C. H. *J. Chem. Soc., Dalton Trans.* **1973**, 1388.
 (27) Abraham, R. J.; Loftus, P. "Proton and Carbon-13 NMR Spectroscopy: An Integrated Approach"; Heyden: London, 1973.
 (28) Christensen, K. A.; Miller, P. E.; Minelli, M.; Rockway, T. W.; Ene-mark, J. H. *Inorg. Chim. Acta* **1981**, *56*, L27.

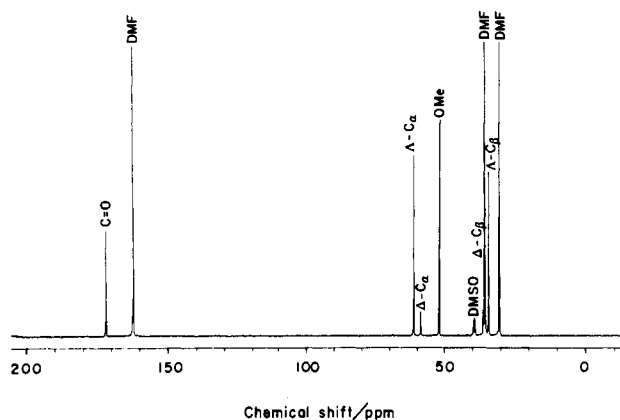


Figure 4. Broad-band proton-decoupled, ¹³C NMR spectrum of [MoO₂(L-cysOMe)₂] recorded at 100 MHz in DMF/Me₂SO-*d*₆ (4:1) at 24 °C.

Table VI. ¹³C NMR Data^a for [MoO₂(L-cysOR)₂] (R = Me or Et) Complexes^b

	Λ-[MoO ₂ (L-cysOMe) ₂] ^c	Δ-[MoO ₂ (L-cysOMe) ₂] ^c	Λ-[MoO ₂ (L-cysOEt) ₂] ^d
C _α	61.47	59.97	61.26 ^f
C _β	34.25	36.10	33.82
CO ₂	172.25	172.48	171.60
R(CH ₃)	52.19 ^e	52.19 ^e	13.99
R(CH ₂)			61.04 ^f

^a Recorded in DMF/Me₂SO-*d*₆ in downfield ppm from Me₄Si (4:1) at 24 °C. ^b Cf. 20-MHz data for cysOR·HCl in D₂O at 24 °C: R = Me, Et; C_α, 55.27, 55.27; C_β, 24.54, 24.65; CO₂, 169.70, 168.95; R, 54.68, 64.71 (CH₂) and 14.19 (CH₃) ppm. ^c 100-MHz spectrum. ^d 20-MHz spectrum. ^e Not resolved. ^f The close proximity of these resonances precludes an unambiguous assignment; they may be reversed.

terminal oxo group (H···O ~ 2.7 Å), whereas the closest intermolecular contacts for the other proton (H_{N'}) are H_α and the symmetry-related amine proton (H_N) on the adjacent N atom.

(ii) ¹³C Spectra. The broad-band proton-decoupled ¹³C NMR spectrum of [MoO₂(L-cysOMe)₂] recorded at 100 MHz in DMF/Me₂SO-*d*₆ (4:1) at 24 °C appears in Figure 4 and the resonance positions are summarized in Table VI. Consistent with this material's ¹H NMR spectrum, two sets of resonances due to a major and minor species, assigned as Λ- and Δ-[MoO₂(L-cysOMe)₂], respectively, were observed. For Λ-[MoO₂(L-cysOMe)₂], the carbonyl resonance appeared at 172.25 ppm, C_α at 61.47 ppm, C_β at 34.25 ppm, and the ester methyl resonance at 52.19 ppm. The Δ-[MoO₂(L-cysOMe)₂] resonances observed were carbonyl carbon at 172.48 ppm, C_α at 59.97 ppm, and C_β at 36.10 ppm; no resonance due to the ester substituent was observed, presumably because this is coincident with the analogous resonance of the Λ isomer. Relative integrations of the two sets of peaks were ca. 5:1 in favor of the major isomer, Λ-[MoO₂(L-cysOMe)₂], again consistent with the ¹H NMR results. The corresponding spectrum of [MoO₂(L-cysOEt)₂], recorded at 20 MHz, showed the resonances listed in Table VI. Consistent with the ¹H NMR data, only one isomer was detected. The C_β (33.82 ppm), carbonyl (171.60 ppm), and ethyl ester (-OCH₂CH₃, 13.99 ppm) resonances can be assigned with confidence; these assignments were confirmed by off-resonance proton-decoupling measurements, where they appeared as a triplet, singlet, and quartet, respectively. The close proximity of the two peaks at 61.04 and 61.26 ppm precludes a definitive assignment of these resonances to the C_α or ester methylene (-OCH₂CH₃) carbon atoms.

As compared to the ¹³C spectra of the ligand hydrochlorides in D₂O at 24 °C, with the exception of the R group resonances

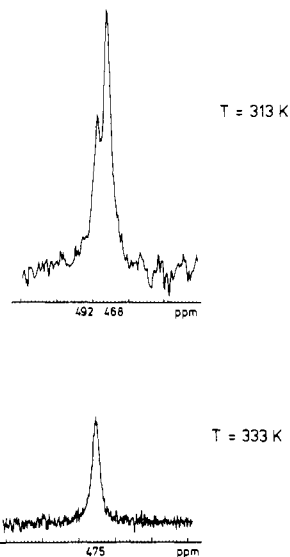


Figure 5. Temperature dependence of ⁹⁵Mo NMR spectra of [MoO₂(L-cysOMe)₂] recorded at 16.3 MHz in DMF solution: top, T = 313 K; bottom, T = 333 K. Each spectrum contains 50 000 scans.

that move slightly (0.2–3.7 ppm) upfield, the resonances move downfield. However, in contrast to the ¹H NMR results, the major effect is for the C_β atom, the displacement being 9.2–11.0 ppm downfield, as compared to the corresponding shifts for the C_α atom, 4.7–6.2 ppm, and carboxylate carbon atom, 2.6–2.8 ppm.

(iii) ⁹⁵Mo Spectra. The ⁹⁵Mo NMR spectra of [MoO₂(L-cysOMe)₂] are reproduced in Figure 5. At 313 K two resonances were observed at 495 and 467 ppm with relative integrations of ca. 1:5. These results are consistent with the ¹H and ¹³C NMR data. Thus the lower field resonance is assigned to the Δ and the higher field resonance to the Λ diastereomer, respectively.

⁹⁵Mo NMR spectra of [MoO₂(L-cysOEt)₂] in Me₂SO, DMF, MeCN, acetone, and MeOH show one peak at 469 ppm (320 K in DMF) with the possibility of an unresolved shoulder at lower field. The ⁹⁵Mo NMR chemical shifts of these complexes are in the range (450–600 ppm) established²⁸ for *cis*-dioxomolybdenum(VI) complexes with a N₂S₂ set of donor atoms.

The temperature dependence of the ⁹⁵Mo NMR spectrum of [MoO₂(L-cysOMe)₂] (Figure 5) shows reversible behavior, with the resonances assigned to the Λ and Δ diastereoisomers coalescing at ca. 333 K. Using expression 2²⁷ where T_c is the

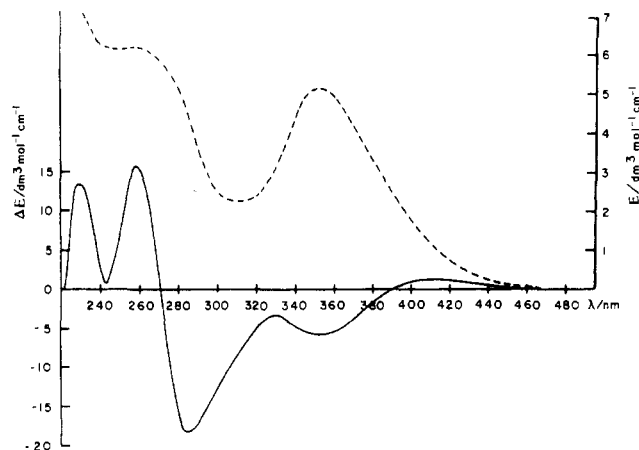
$$\Delta G^* / RT_c = 22.96 + (\ln T_c) / \Delta\nu \quad (2)$$

coalescence temperature (K) and Δν is the frequency separation (in Hz) of the two coalescing lines in the absence of exchange leads to a value of ΔG* for the inversion of configuration (Δ ↔ Λ) about the molybdenum in [MoO₂(L-cysOMe)₂] of 64 kJ mol⁻¹. We are aware that this value is only approximate for a number of reasons, including the following: (i) Equation 2 is derived for exchange between sites of equal population, whereas the relative population of the Λ and Δ diastereoisomers is ca. 5:1. (ii) For quadrupolar nuclei, such as ⁹⁵Mo, the line width of the resonance may be temperature dependent. However, the value of ΔG* obtained here compares reasonably well with that (74 ± 6 kJ mol⁻¹) obtained²³ for the interconversion of Δ- and Λ-[MoO₂(D-penOMe)₂] by ¹H NMR spectroscopy. (iii) ⁹⁵Mo chemical shifts usually increase with increasing temperature.

These ⁹⁵Mo NMR data demonstrate the utility of this spectroscopy not only for discriminating between molybdenum complexes of a very similar nature¹⁰ but also as a means of monitoring interconversions between suitable systems.

Table VII. UV-Visible and CD Spectra of $[\text{MoO}_2(\text{L-cysOR})_2]$ (R = Me or Et)

complex	solvent	spectrum	λ/nm ($10^{-3}\epsilon$ or $\Delta\epsilon/\text{L mol}^{-1}\text{cm}^{-1}$)			
			band 1	band 2	band 3	band 4
$[\text{MoO}_2(\text{L-cysOMe})_2]$	MeCN	UV-vis	352 (5.2)		259 (6.2)	
	MeCN	CD	413 (+1.0)	353 (-4.7)	284 (-14.6)	268 (+12.6)
$[\text{MoO}_2(\text{L-cysOEt})_2]$	Me_2SO	CD	415 (+1.2)	362 (-2.8)	290 (-16.5)	
	MeCN	UV-vis	350 (5.0)		257 (6.1)	
	MeCN	CD	415 (+1.0)	353 (-5.0)	283 (-14.3)	260 (+12.8)
	Me_2SO	CD	415 (+1.4)	360 (-2.2)	290 (-14.9)	...

Figure 6. UV-visible and CD spectra of $[\text{MoO}_2(\text{L-cysOMe})_2]$ in MeCN.

UV-Visible and CD Spectra. The UV-visible and CD spectra of solutions of $[\text{MoO}_2(\text{L-cysOR})_2]$ (R = Me or Et) have been obtained, the details are summarized in Table VII, and the UV-vis and CD spectra of $[\text{MoO}_2(\text{L-cysOMe})_2]$ in MeCN are compared in Figure 6. The complexes display similar electronic absorption spectra with two absorptions being observed at ca. 350 and 260 nm.⁷

The optical activities of these complexes are also very similar, and CD transitions are observed at ca. 410, 350, 285, and 265 nm. Thus, as shown for molybdenum(V) dimers²⁹ and dioxomolybdenum(VI) Schiff base complexes,³⁰ the application of CD spectroscopy allows the resolution of transitions merged under the broad-band envelopes of the absorption spectrum. The CD spectrum arises as the net effect of the spectra of the

Λ and Δ isomers; hence the similar CD profiles are taken to indicate that both of these ester complexes have the same majority isomer, Λ .

Conclusions. Coordination of L-cysOMe to dioxomolybdenum(VI) leads to crystallization of Λ - $[\text{MoO}_2(\text{L-cysOMe})_2]$. In the solid state the complex exhibits the usual distorted octahedral geometry with cis oxo groups, trans thiolate groups, and cis amine groups. In solution two isomers are observed in ca. 5:1 ratio by NMR spectroscopy; these isomers are most reasonably assigned to be the Λ and Δ diastereoisomers of the $\text{MoO}_2(\text{S},\text{N})_2$ complex. The ⁹⁵Mo NMR spectrum coalesces at ca. 333 K, which gives ΔG^\ddagger for their interconversion of ca. 64 kJ mol⁻¹. The CD spectrum of $[\text{MoO}_2(\text{L-cysOMe})_2]$ resolves each of the absorptions at ca. 352 and 259 nm in the UV-visible spectrum into two components. These investigations of the structure and spectroscopic properties of $[\text{MoO}_2(\text{L-cysOMe})_2]$ show that these formally d⁰ complexes exhibit a rich stereochemistry and electronic spectroscopy that has not been previously appreciated. The properties of related dioxomolybdenum(VI) complexes and the relationship of the behavior observed for those complexes to molybdoenzymes are under investigation.

Acknowledgment. We thank Dr. Brian Mann, Dr. K. A. Christensen, and T. W. Rockway for assistance with ⁹⁵Mo NMR spectra. Support of portions of this work by the National Institute of Environmental Health Sciences (Grant ES 0966), the United States Department of Agriculture (Grant 81-CRCR-1-0626), and the North Atlantic Treaty Organization is gratefully acknowledged. I.B. thanks the SERC for a studentship.

Registry No. Λ - $[\text{MoO}_2(\text{L-cysOMe})_2]$, 88269-16-3; Δ - $[\text{MoO}_2(\text{L-cysOMe})_2]$, 88270-64-8; Λ - $[\text{MoO}_2(\text{L-cysOEt})_2]$, 88269-17-4.

Supplementary Material Available: Listings of structure factors, anisotropic thermal parameters for non-hydrogen atoms, and atomic coordinates for hydrogen atoms (7 pages). Ordering information is given on any current masthead page.

(29) Buchanan, I.; Garner, C. D., submitted for publication.

(30) Sullotti, M.; Pasini, A.; Zanderighi, G. M.; Ciani, G.; Sironi, A. J. *Chem. Soc., Dalton Trans.* 1981, 902.